

# Constraints on large- $x$ parton distributions from new weak boson production and deep-inelastic scattering data

(Dated: August 24, 2015)

## Abstract

We present a new set of leading twist parton distribution functions (PDFs), which take advantage of developments in the theoretical treatment of nuclear corrections as well as new data. The analysis includes for the first time data on the free neutron structure function from the BONuS experiment at Jefferson Lab, and new charged lepton and  $W$ -boson asymmetry data from Fermilab, which significantly reduce the uncertainty on the  $d/u$  ratio at large values of  $x$ .

## I. INTRODUCTION

... general intro ...

... what is new since CJ12 ...

• more complete/consistent/systematic treatment of nuclear corrections esp. nucleon off-shell corrections

• impact of new  $W$ -boson asymmetry data on  $d/u$  ratio

• inclusion of JLab (BONuS) data

• analysis of  $\bar{d} - \bar{u}$  at large  $x$  ... choose either  $\bar{d}/\bar{u} \rightarrow 1$  or  $0$  as  $x \rightarrow 1$  ...

• S-ACOT scheme for heavy quarks

• LO fit

•  $\alpha_s$  treatment

... In Sec. II we ...

## II. THEORETICAL FOUNDATIONS

In this section we present the theoretical framework that is used for the CJ15 analysis.

### A. PDF parametrizations

• For the parametrization of the PDFs at the input scale  $Q_0^2$ , a common form has been adopted for all parton species  $f$ ,

$$xf(x, Q_0^2) = a_0 x^{a_1} (1-x)^{a_2} (1 + a_3 \sqrt{x} + a_4 x). \quad (1)$$

This form applies to the valence distributions  $xq_v \equiv x(q - \bar{q})$ , for  $q = u$  and  $d$ , the isoscalar and isovector sea quark distributions  $x(\bar{u} + \bar{d})$  and  $x(\bar{d} - \bar{u})$ , and the gluon distribution  $xg$ . However, to allow for a more flexible parametrization of the valence  $d_v$  PDF in the large- $x$  region, we add in a small admixture of the  $u_v$  PDF,

$$d_v \rightarrow a_0^{d_v} \left( \frac{d_v}{a_0^{d_v}} + b x^c u_v \right), \quad (2)$$

with  $b$  and  $c$  as two additional parameters. The result of this modification is that  $d_v/u_v \rightarrow a_0^{d_v} b$  as  $x \rightarrow 1$ , provided  $a_2^{d_v} > a_2^{u_v}$ , which is usually the case. A finite, nonzero value of this ratio is indeed expected in several nonperturbative models of hadron structure [6–8]. It is

also required from a purely practical point of view, as it avoids potentially large biases on the  $d$ -quark PDF central value [14], as well as on its PDF error estimate, as we discuss in detail in Sec. IV. The  $a_0$  parameters for the  $u_v$  and  $d_v$  distributions are fixed by the appropriate valence quark number sum rules, while  $a_0^g$  is fixed by the momentum sum rule.

- For the input scale  $Q_0$  we choose the charm quark scale,  $Q_0 = m_c$ .
- New parametrization for  $\bar{d} - \bar{u}$  ... avoids negative PDFs? ...

In our analysis we parametrize the  $\bar{d}/\bar{u}$  ratio as

$$\frac{\bar{d}}{\bar{u}} = a_0 x^{a_1} (1-x)^{a_2} + 1 + x^{a_3} (1-x)^{a_4}, \quad (3)$$

which ensures that in the limit  $x \rightarrow 1$  one has  $\bar{d}/\bar{u} \rightarrow 1$ . The existing data are not able to reliably determine the large- $x$  behavior of the ratio, so as an alternative we also perform fits using  $\bar{d}/\bar{u} = a_0 x^{a_1} (1-x)^{a_2} + (1+x^{a_3})(1-x)^{a_4}$ , which vanishes in the  $x \rightarrow 1$  limit. The  $\bar{d}/\bar{u} \rightarrow 1$  limit is what would be expected from perturbative QCD, while the  $\bar{d}/\bar{u} \rightarrow 0$  limit may arise if the trend in  $x \gtrsim 0.3$  points from the E866 experiment [28] were to continue to larger  $x$ .

• The strange quark distribution is not well constrained by existing data ...[SOME DISCUSSION OF ISSUES]... For the strange quark PDF, we follow our previous analyses [14, 15] by assuming flavor independence of the shape of the sea quark PDFs, and consequently take a fixed ratio

$$\kappa = \frac{s + \bar{s}}{\bar{u} + \bar{d}}, \quad (4)$$

with the further assumption that  $\bar{s} = s$ . In this study we take  $\kappa = 0.4$ .

## B. Heavy quarks

- Implementation of S-ACOT scheme.
- In our analysis we take the masses of the charm and bottom quarks to be  $m_c = 1.3$  GeV and  $m_b = 4.5$  GeV, respectively.
- The 4-flavor value of the QCD cutoff scale used in this analysis is  $\Lambda_{\text{QCD}}^{(4)} = 226.8$  MeV.

### C. $1/Q^2$ corrections

- For target mass corrections, use of OPE (G-P); ... comparisons with EFP, series expansion; ... in practice doesn't matter! (?)
- For other subleading  $1/Q^2$  corrections, such as higher twist and other residual power corrections (
- ... anything different to CJ12??

$$F_2(x, Q^2) = F_2^{\text{LT}}(x, Q^2) \left( 1 + \frac{C(x)}{Q^2} \right), \quad (5)$$

where  $F_2^{\text{LT}}$  denotes the leading twist structure function including TMCs. For simplicity we generically refer to the fitted  $1/Q^2$  term as a “higher twist” correction, and parametrize the higher twist coefficient function by

$$C(x) = h_0 x^{h_1} (1 + h_2 x), \quad (6)$$

assuming it to be isospin independent (see, however, Refs. [60–63]).

### D. Nuclear corrections

- The analysis includes nuclear corrections for deuterium account for nucleon Fermi motion and nuclear binding effects, which are implemented using nuclear smearing functions, as well as rescattering effects mediated by Pomeron and meson exchange mechanisms which give rise to shadowing at small  $x \lesssim 0.1$  and a small amount of antishadowing at  $x \sim 0.1$ . For the shadowing and antishadowing corrections, the model of Ref. [1] is used (see also Refs. [2, 3]), although the effects of these is negligible in our analysis.

The implementation of the nuclear smearing is performed ... ..

#### 1. Nuclear smearing

Since nucleons bound in a nucleus are not free, the nuclear structure function deviates from a simple sum of free proton and neutron structure functions, especially at large  $x$  where the effects of Fermi motion, nuclear binding, and nucleon off-shellness are most prominent. In the nuclear impulse approximation the structure function of the deuteron  $d$  can be expressed

as a generalized convolution of the bound nucleon structure function and a momentum distribution  $f_{N/d}$  of nucleons in the deuteron [64, 65],

$$q^d(x, Q^2) = \int \frac{dz}{z} dp^2 f_{N/d}(z, p^2) \tilde{q}^N(x/z, p^2, Q^2), \quad (7)$$

where  $f_{N/d}(z, p^2)$  gives the (light-cone) distribution of nucleons in the deuteron for a given nucleon momentum fraction in the deuteron  $z = (M_d/M)(p \cdot q / p_d \cdot q)$  and nucleon virtuality  $p^2$ , where  $p$  and  $p_d$  are the four-momenta of the nucleon and deuteron, respectively, and  $M_d$  is the deuteron mass. The function  $\tilde{q}^N$  is the off-shell nucleon structure function, and a sum over the nucleons  $N = p, n$  is implied. ... The function  $\tilde{q}^N$  includes  $1/Q^2$  corrections, such as TMCs and higher twist effects. ... Expanding the off-shell nucleon structure function about the on-shell limit, one finds [66]

$$\tilde{q}^N(x, p^2, Q^2) = q^N(x, Q^2) \left( 1 + \frac{p^2 - M^2}{M^2} \delta f^N(x, Q^2) \right), \quad (8)$$

where the coefficient of the off-shell term is

$$\delta f^N(x, Q^2) = \left. \frac{\partial \ln \tilde{q}^N(x, p^2, Q^2)}{\partial \ln p^2} \right|_{p^2=M^2}, \quad (9)$$

and the  $\tilde{q}^N$  includes the parametrized higher twist corrections of Eq. (5). The on-shell term leads to the standard on-shell convolution representation for the nuclear structure function, while the off-shell term can be evaluated as an additive correction,  $q^d = q^{d(\text{on})} + q^{d(\text{off})}$ , where

$$q^{d(\text{on})}(x, Q^2) = \int \frac{dz}{z} f^{(\text{on})}(z) q^N(x/z, Q^2), \quad (10a)$$

$$q^{d(\text{off})}(x, Q^2) = \int \frac{dz}{z} f^{(\text{off})}(z) \delta f^N(x/z, Q^2) q^N(x/z, Q^2). \quad (10b)$$

The on-shell and off-shell smearing functions  $f^{(\text{on})}$  and  $f^{(\text{off})}$  are taken to be the same for the proton and neutron, and are given by [68]

$$f^{(\text{on})}(z) = \int dp^2 f_{N/d}(z, p^2), \quad (11a)$$

$$f^{(\text{off})}(z) = \int dp^2 \frac{p^2 - M^2}{M^2} f_{N/d}(z, p^2). \quad (11b)$$

The momentum distributions, or “smearing functions”,  $f^{(\text{on})}$  and  $f^{(\text{off})}$ , are computed in the weak binding approximation (WBA) in terms of the deuteron wave function, and include the effects of nuclear binding and Fermi motion [66, 67]. At  $Q^2 \rightarrow \infty$  the on-shell smearing

function  $f^{(\text{on})}$  has a simple probabilistic interpretation in terms of the light-cone momentum fraction  $z \approx (M_d/M)(p^+/p_d^+)$  of the deuteron carried by the struck nucleon, while at finite  $Q^2$  it depends in addition on the parameter  $\rho^2 = 1 + 4x^2 M^2/Q^2$ , which characterizes the deviation from the Bjorken limit.

The nuclear corrections at large  $x$  depend partly on the strength of the high-momentum tail of the deuteron wave function, and we use several wave functions based on different nucleon–nucleon potentials to study the deuteron model dependence. We choose the high-precision AV18 [69], CD-Bonn [70] and the relativistic WJC-1 and WJC-2 [71] wave functions, which provide a representative spread of behaviors at high momentum. Note that the effects of the nuclear smearing corrections are not suppressed at large  $Q^2$ , and must be considered at all scales wherever data at  $x \gtrsim 0.3$  are used [11–13].

- Same off-shell functions in DIS and DY.

## 2. Nucleon off-shell corrections

- The off-shell nucleon correction  $\delta^{(\text{off})} q^d$  is somewhat more model dependent, but several quark model based estimates of this have been made in the literature [66, 72, 73].

- ... give brief history of off-shell corrections
  - MST (theoretical)
  - KP (model/fitted)
  - CJ11 (mKP)
  - CJ12 (more consistent mKP)
  - CJ15 (calculation at parton level - different treatment of valence quarks, antiquarks and gluons - can apply to any observable, not just  $F_2$  structure function - in CJ11 and CJ12 had used overall multiplicative constant, only for  $F_2$ )

- In Ref. [14] this was computed using the “modified Kulagin-Petti” model. In this model, the corrections were related to the change in the nucleon’s confinement radius in the nuclear medium, as well as the average virtuality of the bound nucleons, and constrained to give no net change in the structure function normalization. In contrast to Ref. [14], however, here we further take into account the correlation between the nucleon “swelling” and the deuteron wave function. The combined effects introduce a theoretical uncertainty in the extracted PDFs, particularly for the  $d$  quark.

- In CJ15 have freed off-shell parameters, allowing them to be determined by the fit. Using either fmKP model (rescaling parameter  $\lambda$ ), or in phenomenological fit.

- In this analysis, we explore the possibility of antishadowing in the deuteron, suggested in the global nuclear analysis of KP [66], in which the  $F_2^d/F_2^N$  ratio is slightly enhanced (above unity) at  $x \approx 0.1 - 0.2$ . To allow for one or more zero crossings in the function  $\delta f^N$ , we use the same parametrization as in Ref. [66],

$$\delta f^N = C_N(x - x_0)(x - x_1)(x - x_2), \quad (12)$$

but fit the parameters to the deuterium data. The requirement that the off-shell correction does not modify the number of valence quarks in the nucleon provides the constraint

$$\int_0^1 dx \delta f^N(x) (q(x) - \bar{q}(x)) = 0. \quad (13)$$

### E. PDF Errors

... as for CJ12 ... Hessian ... tolerance ...

## III. DATA

The CJ15 PDFs are obtained by fitting to a global database of 4035 data points from a variety of high energy scattering processes, listed in Table I. These include deep-inelastic scattering data from BCDMS, NMC, SLAC, HERA and Jefferson Lab (JLab); Drell-Yan  $p$  and  $d$  cross sections from fixed target experiments at Fermilab;  $W$  and  $Z$  asymmetries, as well as jet and  $\gamma$ +jet cross sections from the CDF and DØ collaborations at the Tevatron. The table also lists the corresponding  $\chi^2$  values for each data set. The overall  $\chi^2/\text{dof}$  is 0.979. The fit is slightly better than in our previous CJ12 analysis [15], partly because of the greater flexibility which we have allowed in the current fit for the nucleon off-shell correction.

...[FURTHER DESCRIPTIONS OF DATA]... ...[JUSTIFICATION FOR INCLUDING AND OMITTING SPECIFIC DATA SETS]...

## IV. RESULTS

In this section we present the results of our global QCD analysis. The quality of the fit to data is illustrated in Figs. 1 and 2, where the inclusive  $F_2$  structure functions of the proton and deuteron are compared with the CJ15 calculations over several decades of  $Q^2$  and  $x$ . For the proton  $F_2^p$  structure function in Fig. 1, data from BCDMS [22], NMC [23], SLAC [25] and JLab [26] experiments are shown at approximately constant values of  $x$ , while for the JLab data (see inset in Fig. 1) the structure functions are presented at fixed scattering angles, with  $x$  increasing with  $Q^2$ . The agreement for all the sets is excellent ...[???]..., with the exception of ...[???]...

Similar agreement is seen for the deuteron  $F_2^d$  structure function in Fig. 2, where measurements from BCDMS [22], SLAC [25] and JLab [26] are compared with the CJ15 results (data from NMC are presented as a ratio to the proton structure function,  $F_2^d/F_2^p$ ). ...[SHOW OTHER, e.g. HERA, DATA SEPARATELY??]...

### A. CJ15 PDFs

The CJ15 PDFs themselves are displayed in Fig. 3 at a scale of  $Q^2 = 10 \text{ GeV}^2$  for the  $u$ ,  $d$ ,  $\bar{d} + \bar{u}$  and  $\bar{d} - \bar{u}$  distributions, and the gluon distribution scaled by a factor 1/10. The central CJ15 PDFs are determined using the AV18 deuteron wave function and the nucleon off-shell parametrization in Eq. (12), with the parameter values for the leading twist distributions given in Table II. at the input scale  $Q_0^2$ . The uncertainty bands on the PDFs correspond to  $\Delta\chi^2 = 1$ . PDFs for other flavors, such as strange and charm, are not shown in Fig. 3. The strange quark PDF is assumed to be proportional to the light antiquark sea in the ratio  $\kappa = 0.4$  [see Eq. (4)], while the charm quark distribution is generated perturbatively through  $Q^2$  evolution. While there has been speculation about nonperturbative or intrinsic contributions to PDFs of heavy flavors, there is currently no evidence from global analysis of high energy scattering data to suggest that these are large [? ]. Until more conclusive evidence becomes available, in this analysis we follow the conventional approach in setting these to zero. This is in contrast with the light quark sea, for which a nonperturbative component at the input scale is essential to account for the nonzero flavor asymmetry  $\bar{d} - \bar{u}$ . ...[NOTE VERY ASYMMETRIC ERRORS AT SMALL  $x$ ]...



The CJ15 PDFs are compared with PDFs from several recent representative NLO global parametrizations in Fig. 4, in the form of ratios to the central CJ15 distributions. Since different PDF analyses typically utilize different criteria for estimating PDF errors, we display the CJ15 errors for the standard  $\Delta\chi^2 = 1$  (or tolerance  $T = 1$ ), as well as with errors inflated by a tolerance of  $T = 10$  [15]. Generally the MMHT14 [17] and NNPDF3.0 [19] PDF sets have uncertainties that are comparable to the CJ15 PDF errors with  $T = 10$ , while those for the HERAPDF15 [21] distributions are closer to the CJ15  $T = 1$  errors. This may be expected given that the HERAPDF15 analysis only fits HERA data, and therefore uses the  $\Delta\chi^2 = 1$  criterion for generating errors.

As observed in most previous analyses, the relative uncertainties on the  $d$ -quark PDFs are significantly larger than those on the  $u$ -quark PDF, especially at large  $x$ . For the  $\bar{u}$  and  $\bar{d}$  distributions

- \* HERAPDF15  $\bar{d} - \bar{u}$  is not constrained. most strongest constr. from E866 pd/pp DY data.

- \* strange CJ15 errors smaller than others; CJ15  $s$  is assumed to scale with the light antiquark sea in the ratio  $\kappa = 0.4$ , while other analyses attempt to constrain  $s$ -quark PDF from neutrino data, which typically have much larger uncertainties.

- \* gluon errors at small  $x$  for MMHT and NNPDF lie somewhere between the  $T = 1$  and  $T = 10$  CJ15 errors... larger- $x$  data ???

The uncertainty on the  $d$ -quark distribution is generally much smaller at large  $x$  ( $x \gtrsim 0.3$ ) compared with the  $u$ . This reflects the greater availability of the proton  $F_2^p$  structure function data, which because of the larger charge on the  $u$  quark is an order of magnitude more sensitive to the  $u$ -quark PDF than to the  $d$ . Traditionally, greater sensitivity to the  $d$ -quark PDF is obtained from inclusive DIS from the neutron, in which the roles of the  $u$  and  $d$  quark are reversed relative to the proton. However, the absence of free neutron targets has meant that neutron structure information has had to be extracted from measurements on the deuteron. Unfortunately, at high values of  $x$  ( $x \gtrsim 0.5$ ) bound state effects in the deuteron become important, and uncertainties in their computation increase with increasing  $x$ .

- \* uncertainty on  $d$  much larger at high  $x$  than on  $u$

- \* MMHT14 uncertainties are typical of other modern global fits, such as CT14 [18] or NNPDF3.0 [19].

\* other features worth discussing?

In Table II the initial parameter values for the leading twist CJ15 PDFs and their errors are listed. The parameters without errors have been fixed by sum rules or other constraints. (To avoid rounding errors when using these values in numerical calculations, we give the parameter values to 5 significant figures.) The parameters for the higher twist correction to  $F_2$  in Eqs. (5) and (6), as well as the nucleon off-shell parameters in Eq. (12), are given in Table III.

### B. Nuclear corrections at large $x$

The effects of nuclear corrections on the PDFs are illustrated in Fig. 6, where several different deuteron wave function models have been used in the fits. The distributions are displayed relative to the central CJ15 PDFs which use the AV18 deuteron wave function. The results using the CD-Bonn or WJC-2 wave function are very similar to those for the AV18 wave function, while using the WJC-1 model leads to larger differences. This suggests that, for the most part, the nucleon off-shell parametrization in Eq. (12) is sufficiently flexible so as to be able compensate for changes induced by the different wave functions. For the WJC-1 wave function, which has the hardest momentum distribution, it is more difficult for the off-shell correction to compensate. Recall from Table I that the AV18, CD-Bonn and WJC-2 models give the lowest values of  $\chi^2/\text{dof}$  (...), while the WJC-1 model gives the largest value.

As expected, the variations due to the nuclear models have the largest effects in the  $d$ -quark distribution, which is less constrained by proton data and hence more sensitive to uncertainties in the extracted neutron structure function. The spread in the  $d$  PDF at  $x = 0.8$  is  $\approx 20\%$  for the various wave functions. The variations for the AV18, CD-Bonn and WJC-2 wave functions are generally within the  $\Delta\chi^2 = 1$  confidence limit, while the WJC-1 results lie outside the band for the  $u$  and  $d$  PDFs. Interestingly, one observes an anti-correlation between the behavior of the  $d$ -quark distribution at large  $x$  and the gluon distribution. In fact, using the WJC-1 wave functions leads to slight decreases in all the quark PDFs at high  $x$ , while the gluon PDF has the opposite trend. The spread in the gluon PDF is  $\lesssim 10\%$  for  $x < 0.8$ , although beyond  $x \approx 0.3$  the gluon distribution has a very large uncertainty.

Using the 1-parameter off-shell rescaling model (ORM) for the nucleon off-shell corrections, the corresponding PDF ratios are displayed in Fig. 8. For the AV18, CD-Bonn and WJC-2 wave functions, the effects of using the more flexible off-shell parametrization (12) and the more restrictive ORM form are very small, and generally within the  $\Delta\chi^2 = 1$  bands. For the WJC-1 wave function, the results for the  $d$ -quark PDF show significantly greater deviation at large  $x$ , again suggesting that the off-shell rescaling model is not able to compensate for the hard tail of its momentum distribution. In addition, for the  $u$ -quark distribution the WJC-1 result lies slightly outside the uncertainty band at  $x \sim 0.05$ .

### C. $d/u$ ratio

The impact of the nuclear corrections and data constraints on the  $d/u$  ratio are illustrated in Figs. 12 and 13.

In Fig. 12:

- BONuS data shrink error on  $d/u$  slightly in the  $x \approx 0.5 - 0.6$  range
- significant reduction in error once  $W$  asymmetry data added
- For other deuteron wave function models, the total  $\chi^2$  values are very similar, with  $\chi^2/\text{dof} = 0.979$  for the CD-Bonn wave function, 0.983 for the WJC-1 wave function, and 0.980 for the WJC-2 model. The AV18, CD-Bonn and WJC-2 model fits are therefore essentially indistinguishable, while the WJC-1 model, with its significantly harder deuteron wave function, has a slightly worse overall fit.

• With the off-shell covariant spectator (OCS) model ...[WHAT WE HAD BEEN CALLING “fmKP”]..., the  $\chi^2$  values for the various wave functions are marginally higher, with  $\chi^2/\text{dof} = 0.982, 0.982, 0.989$  and 0.984 for the AV18, CD-Bonn, WJC-1 and WJC-2 models. Here again the WJC-1 gives the worst fit. ...[MORE DISCUSSION]...

- impact of various data sets on  $d/u$  ratio:
  - DIS only: large uncertainty
  - BONuS shrinks uncertainty appreciably at  $x \sim 0.6$
  - lepton asymmetry data gives significant reduction in uncertainty at  $0.2 \lesssim x \lesssim 0.4$ , with smaller reduction at larger  $x$
  - $Z$  rapidity data, on the other hand, has very little effect on the uncertainty
  - $W$  asymmetry data, in particular the DØ data [34], gives significant reduction in the

$d/u$  uncertainty for  $x \gtrsim 0.6$

The effects of deuterium data and the nuclear corrections in the deuterium data are illustrated in Fig. 13:

- with no nuclear corrections the  $d/u$  ratio is larger at  $x \gtrsim 0.6$  than with the nuclear corrections. This can be understood from the shape of the  $F_2^d/F_2^N$  ratio Fig. 5 at large  $x$ , where the effect of the nuclear corrections is to increase the ratio above unity for  $x \gtrsim 0.6$ . Since  $F_2^d$  and  $F_2^p$  are fixed inputs, a larger  $F_2^d/F_2^N$  is generated by a smaller neutron  $F_2^n$  and hence a smaller  $d/u$  ratio. For example, the effect of the nuclear corrections is to shift the  $d/u$  ratio at  $x = 0.8$  from the ( $T = 10$ ) range  $\approx 0.1 - 0.3$  to  $\approx 0 - 0.2$  once the smearing and off-shell effects are included.

- removing the deuterium data altogether increases the overall uncertainty band for  $x \gtrsim 0.7$ . Interestingly, the deuteron data also reduce the  $d/u$  uncertainties slightly at smaller  $x$ ,  $x \lesssim 0.1$ .

The final CJ15  $d/u$  results and uncertainties (for  $T = 10$ ) can be compared with ratios obtained in other recent global PDF analyses. These are shown in Fig. 11 for the MMHT14 [17], CT14 [18] and JR14 [47] PDFs.

- JR14 uses similar experimental data sets and treatment of nuclear and finite- $Q^2$  corrections at large  $x$ ;
- JR14 has largest uncertainty in the intermediate- $x$  region, which may result from the recent  $W$  and lepton asymmetry data from CDF and DØ not being used;
- at large  $x$  the JR14  $d/u$  ratio  $\rightarrow 0$  from the form of their parametrization;
- CT14 range is similar

## V. CONCLUSION

## Acknowledgments

We thank M. E. Christy, P. Monaghan, ... for helpful discussions. This work was supported by the DOE contract No. DE-AC05-06OR23177, under which Jefferson Science Associates, LLC operates Jefferson Lab. The work of J.F.O. and A.A. was supported in part by DOE contracts No. DE-FG02-97ER41922 and No. DE-SC0008791, respectively.

- 
- [1] W. Melnitchouk and A. W. Thomas Phys. Rev. D **47**, 3783 (1993).
  - [2] B. Badelek and J. Kwiecinski, Nucl. Phys. **B370**, 278 (1992).
  - [3] L. P. Kaptari and A. Yu. Umnikov, Phys. Lett. B **272**, 359 (1991).
  - [4] R. P. Feynman, *Photon Hadron Interactions* (Benjamin, Reading, Massachusetts, 1972).
  - [5] F. E. Close, Phys. Lett. B **43**, 422 (1973).
  - [6] G. R. Farrar and D. R. Jackson, Phys. Rev. Lett. **35**, 1416 (1975).
  - [7] W. Melnitchouk and A. W. Thomas, Phys. Lett. B **377**, 11 (1996).
  - [8] R. J. Holt and C. D. Roberts, Rev. Mod. Phys. **82**, 2991 (2010).
  - [9] S. Kuhlmann *et al.*, Phys. Lett. B **476**, 291 (2000).
  - [10] L. T. Brady, A. Accardi, W. Melnitchouk and J. F. Owens, JHEP **1206**, 019 (2012).
  - [11] A. Accardi, M. E. Christy, C. E. Keppel, P. Monaghan, W. Melnitchouk, J. G. Morfin and J. F. Owens, Phys. Rev. D **81**, 034016 (2010).
  - [12] J. Arrington, F. Coester, R. J. Holt and T. -S. H. Lee, J. Phys. G **36**, 025005 (2009).
  - [13] J. Arrington, J. G. Rubin and W. Melnitchouk, Phys. Rev. Lett. **108**, 252001 (2012).
  - [14] A. Accardi, W. Melnitchouk, J. F. Owens, M. E. Christy, C. E. Keppel, L. Zhu and J. G. Morfin, Phys. Rev. D **84**, 014008 (2011).
  - [15] J. F. Owens, A. Accardi and W. Melnitchouk, Phys. Rev. D **87**, 094012 (2013).
  - [16] The CTEQ-Jefferson Lab (CJ) collaboration website, <http://www.jlab.org/cj>.
  - [17] L. A. Harland-Lang, A. D. Martin, P. Motylinski and R. S. Thorne, Eur. Phys. J. C **75**, 204 (2015).
  - [18] S. Dulat *et al.*, arXiv:1506.07443 [hep-ph].
  - [19] R. D. Ball *et al.*, JHEP **1504**, 040 (2015).
  - [20] F. D. Aaron *et al.*, JHEP **1001**, 109 (2010).

- [21] V. Radescu, arXiv:1308.0374.
- [22] A. C. Benvenuti *et al.*, Phys. Lett. B **223**, 485 (1989); *ibid.* B **236**, 592 (1989).
- [23] M. Arneodo *et al.*, Nucl. Phys. B **483**, 3 (1997).
- [24] M. Arneodo *et al.*, Nucl. Phys. B **487**, 3 (1997).
- [25] L. W. Whitlow *et al.*, Phys. Lett. B **282**, 475 (1992).
- [26] S. P. Malace *et al.*, Phys. Rev. C **80**, 035207 (2009).
- [27] F. D. Aaron *et al.*, JHEP **1001**, 109 (2010).
- [28] E. A. Hawker *et al.*, Phys. Rev. Lett. **80**, 3715 (1998); J. Webb, Ph.D. Thesis, New Mexico State University (2002), arXiv:hep-ex/0301031; P. Reimer, private communication, [http://p25ext.lanl.gov/e866/papers/e866dyabs/E866\\_Drell-Yan\\_Cross\\_Sections/E866\\_Drell-Yan](http://p25ext.lanl.gov/e866/papers/e866dyabs/E866_Drell-Yan_Cross_Sections/E866_Drell-Yan)
- [29] R. S. Towell *et al.*, Phys. Rev. D **64**, 052002 (2001).
- [30] D. Acosta *et al.*, Phys. Rev. D **71**, 051104(R) (2005).
- [31] V. M. Abazov *et al.*, Phys. Rev. D **88**, 091102 (2013).
- [32] V. M. Abazov *et al.*, Phys. Rev. D **91**, 032007 (2015).
- [33] T. Aaltonen *et al.*, Phys. Rev. Lett. **102**, 181801 (2009).
- [34] V. M. Abazov *et al.*, Phys. Rev. Lett. **112**, 151803 (2014) [Phys. Rev. Lett. **114**, 049901 (2015)].
- [35] T. Aaltonen *et al.*, Phys. Lett. B **692**, 232 (2010).
- [36] V. M. Abazov *et al.*, Phys. Rev. D **76**, 012003 (2007).
- [37] T. Affolder *et al.*, Phys. Rev. D **64**, 032001 (2001).
- [38] T. Aaltonen *et al.*, Phys. Rev. D **78**, 052006 (2008).
- [39] B. Abbott *et al.*, Phys. Rev. Lett. **86**, 1707 (2001).
- [40] V. M. Abazov *et al.*, Phys. Rev. Lett. **101**, 062001 (2008).  
B. Abbott *et al.*, Phys. Rev. Lett. **86**, 1707 (2001).
- [41] V. M. Abazov *et al.*, Phys. Lett. B **666**, 435 (2008).
- [42] D. Mason *et al.*, Phys. Rev. Lett. **99**, 192001 (2007).
- [43] G. Aad *et al.*, Phys. Rev. Lett. **109**, 012001 (2012).
- [44] G. Moreno *et al.*, Phys. Rev. D **43**, 2815 (1991). ...[IS THIS CORRECT REFERENCE??]...
- [45] S. Alekhin, J. Blümlein and S.-O. Moch, Phys. Rev. D **86**, 054009 (2012).
- [46] A. D. Martin, W. J. Stirling, R. S. Thorne and G. Watt, Eur. Phys. J. C **63**, 189 (2009).
- [47] P. Jimenez-Delgado and E. Reya, Phys. Rev. D **89**, 074049 (2014).

- [48] P. Jimenez-Delgado, W. Melnitchouk and J. F. Owens, J. Phys. G: Nucl. Part. Phys. **40**, 093102 (2013).
- [49] J. Beringer *et al.* [Particle Data Group Collaboration], Phys. Rev. D **86**, 010001 (2012), <http://pdg.lbl.gov>.
- [50] H. Georgi and H. D. Politzer, Phys. Rev. D **14**, 1829 (1976).
- [51] R. K. Ellis, R. Petronzio and G. Parisi, Phys. Lett. B **64**, 97 (1976).
- [52] A. Accardi and J.-W. Qiu, JHEP **0807**, 090 (2008).
- [53] A. Accardi, T. Hobbs and W. Melnitchouk, JHEP **0911**, 084 (2009).
- [54] I. Schienbein *et al.*, J. Phys. G **35**, 053101 (2008).
- [55] L. T. Brady, A. Accardi, T. J. Hobbs and W. Melnitchouk, Phys. Rev. D **84**, 074008 (2011) [Erratum-ibid. D **85**, 039902 (2012)].
- [56] F. M. Steffens and W. Melnitchouk, Phys. Rev. C **73**, 055202 (2006).
- [57] F. M. Steffens, M. D. Brown, W. Melnitchouk and S. Sanches, Phys. Rev. C **86**, 065208 (2012).
- [58] A. De Rújula, H. Georgi and H. D. Politzer, Phys. Rev. D **15**, 2495 (1977).
- [59] A. De Rújula, H. Georgi and H. D. Politzer, Ann. Phys. **103**, 315 (1977).
- [60] M. Virchaux and A. Milsztajn, Phys. Lett. B **274**, 221 (1992).
- [61] S. I. Alekhin, S. A. Kulagin and S. Liuti, Phys. Rev. D **69**, 114009 (2004).
- [62] J. Blümlein and H. Böttcher, Phys. Lett. B **662**, 336 (2008).
- [63] J. Blümlein, Prog. Part. Nucl. Phys. **69**, 28 (2013).
- [64] W. Melnitchouk, A. W. Schreiber and A. W. Thomas, Phys. Rev. D **49**, 1183 (1994).
- [65] S. A. Kulagin, G. Piller and W. Weise, Phys. Rev. C **50**, 1154 (1994).
- [66] S. A. Kulagin and R. Petti, Nucl. Phys. A **765**, 126 (2006).
- [67] Y. Kahn, W. Melnitchouk and S. A. Kulagin, Phys. Rev. C **79**, 035205 (2009).
- [68] P. J. Ehlers, A. Accardi, L. T. Brady and W. Melnitchouk, Phys. Rev. D **90**, 014010 (2014).
- [69] R. B. Wiringa, V. G. J. Stoks and R. Schiavilla, Phys. Rev. C **51**, 38 (1995).
- [70] R. Machleidt, Phys. Rev. C **63**, 024001 (2001).
- [71] F. Gross and A. Stadler, Phys. Rev. C **78**, 014005 (2008); *ibid.* C **82**, 034004 (2010).
- [72] F. Gross and S. Liuti, Phys. Rev. C **45**, 1374 (1992).
- [73] W. Melnitchouk, A. W. Schreiber and A. W. Thomas, Phys. Lett. B **335**, 11 (1994).
- [74] J. Pumplin *et al.*, JHEP **0207**, 012 (2003).
- [75] The CTEQ collaboration website, <http://www.cteq.org>.

- [76] A. D. Martin, A. J. Th. M. Mathijssen, W. J. Stirling, R. S. Thorne, B. J. A. Watt and G. Watt, Eur. Phys. J. C **73**, 2318 (2013).
- [77] A. Accardi, AIP Conf. Proc. **1369**, 210 (2011).
- [78] D. Stump *et al.*, JHEP **0310**, 046 (2003).
- [79] J. Anderson [LHCb Collaboration], arXiv:1109.3371 [hep-ex].
- [80] D. d’Enterria and J. Rojo, Nucl. Phys. **B860**, 311 (2012), arXiv:1202.1762[hep-ph].
- [81] Y. Liang *et al.* [Jefferson Lab Hall C E94-110 Collaboration], arXiv:nucl-ex/0410027.
- [82] P. Monaghan, A. Accardi, M. E. Christy, C. E. Keppel, W. Melnitchouk and L. Zhu, Phys. Rev. Lett. **110**, 152002 (2013).
- [83] N. Baillie *et al.*, Phys. Rev. Lett. **108**, 142001 (2012); S. Tkachenko *et al.*, Phys. Rev. C **89**, 045206 (2014).
- [84] Jefferson Lab Experiment C12-10-103 [MARATHON], G. G. Petratos, J. Gomez, R. J. Holt and R. D. Ransome, spokespersons.
- [85] Jefferson Lab Experiment E12-10-102 [BONUS12], S. Bültmann, M. E. Christy, H. Fenker, K. Griffioen, C. E. Keppel, S. Kuhn and W. Melnitchouk, spokespersons.
- [86] Jefferson Lab Experiment E12-10-007 [SoLID], P. Souder, spokesperson.
- [87] P. Jimenez-Delgado, T. J. Hobbs, J. T. Londergan and W. Melnitchouk, Phys. Rev. Lett. **114**, 082002 (2015).



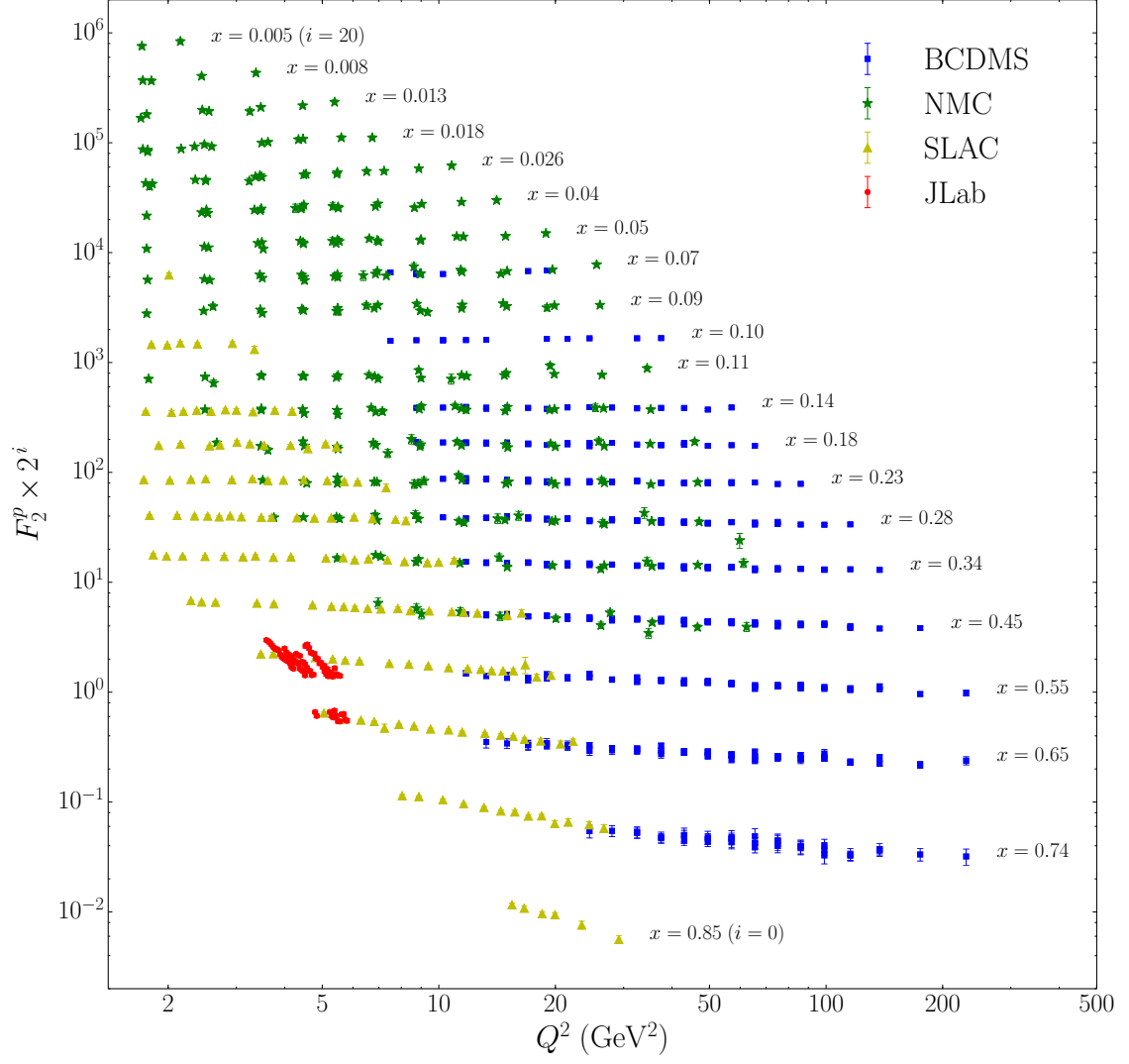


FIG. 1: Comparison of proton  $F_2^p$  structure function data from BCDMS [22], NMC [23], SLAC [25] and JLab [26] with the CJ15 NLO fit, for various  $Q^2$  and  $x$ . The data at fixed  $x$  values have been scaled by a factor  $2^i$ , from  $i = 0$  for  $x = 0.85$  to  $i = 20$  for  $x = 0.005$  in steps of  $i = 1$ .

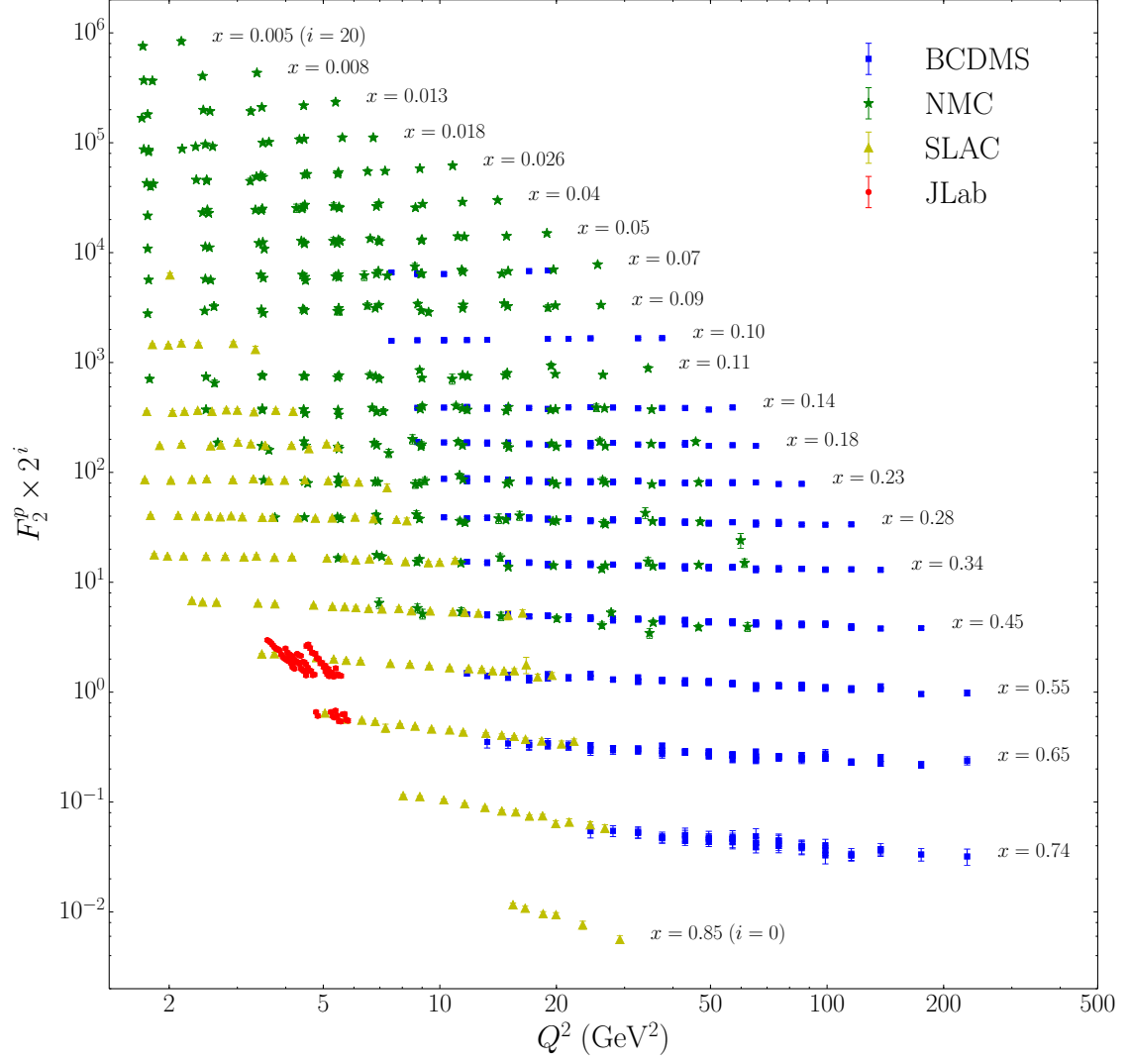


FIG. 2: [PLACEHOLDER FIGURE]... As for Fig. 1, but for the deuteron  $F_2^d$  structure function, illustrating data from BCDMS [22], SLAC [25] and JLab [26]. ...[WHAT TO DO WITH NMC  $F_2^d/F_2^p$  ?]...

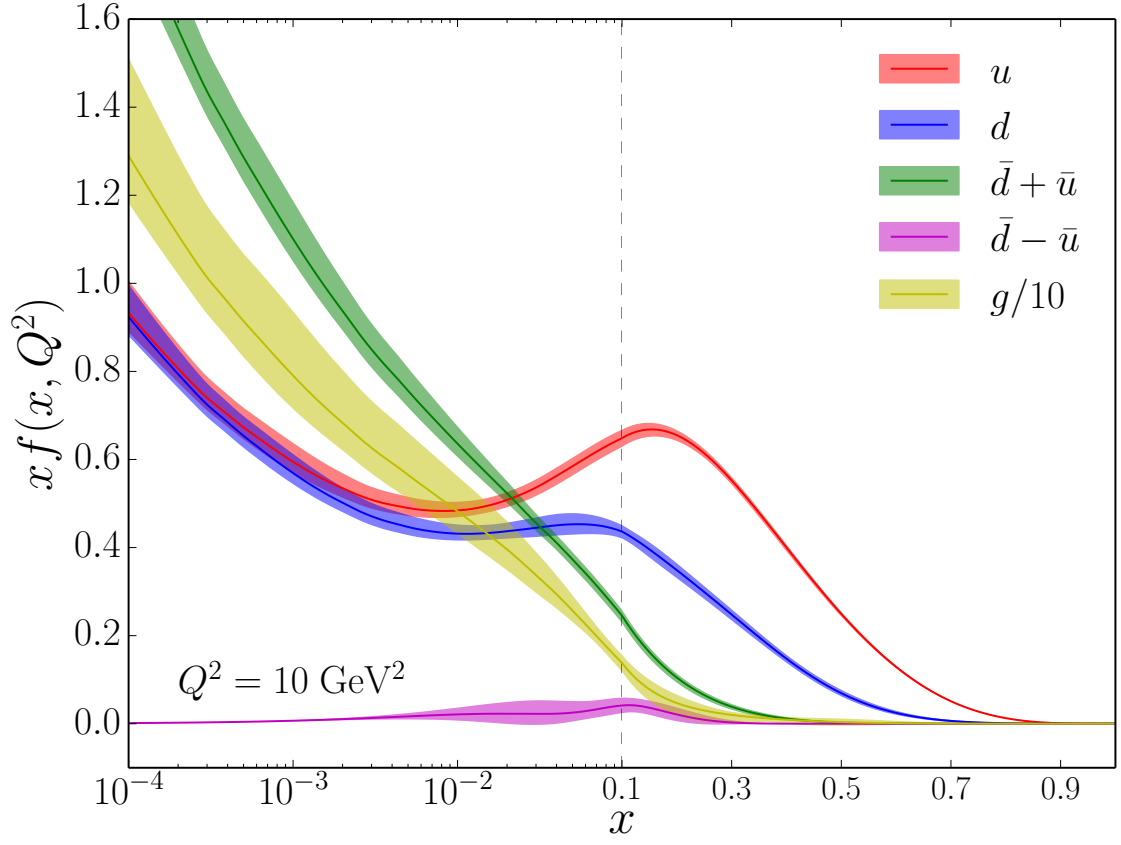


FIG. 3: Comparison of CJ15 PDFs for different flavors ( $u, d, \bar{d} + \bar{u}, \bar{d} - \bar{u}$  and  $g/10$ ) at a scale  $Q^2 = 10 \text{ GeV}^2$ , for  $T = 1$ . Note the combined logarithmic/linear scale along the  $x$ -axis.

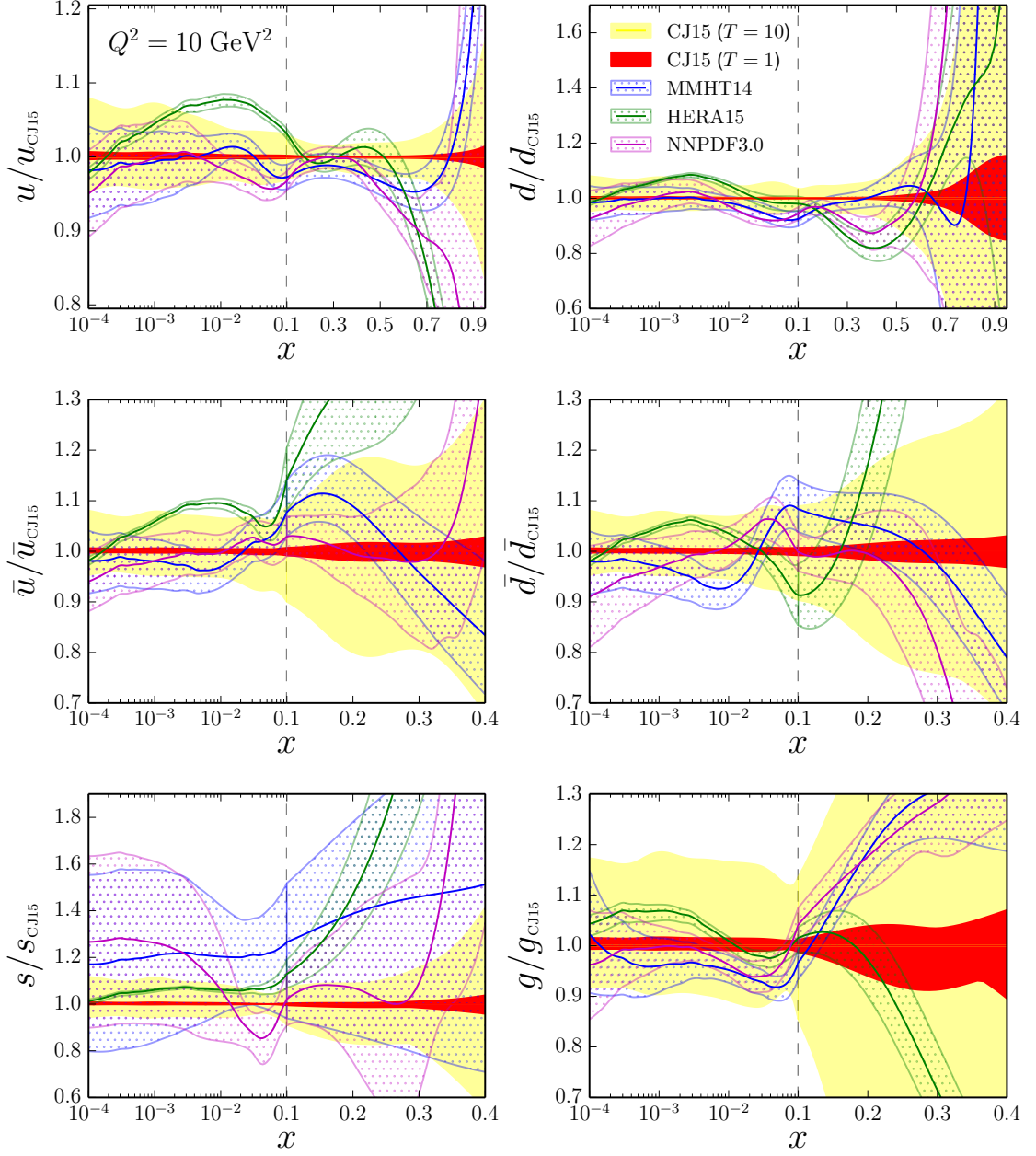


FIG. 4: Ratio of PDFs to the CJ15 central values for various PDF sets: CJ15 for tolerance  $T = 1$  (red) and  $T = 10$  (yellow), MMHT14 [17] (blue), HERAPDF15 [21] (green), and NNPDF3.0 [19] (magenta). Note the different scales on the vertical axes used for different flavors.

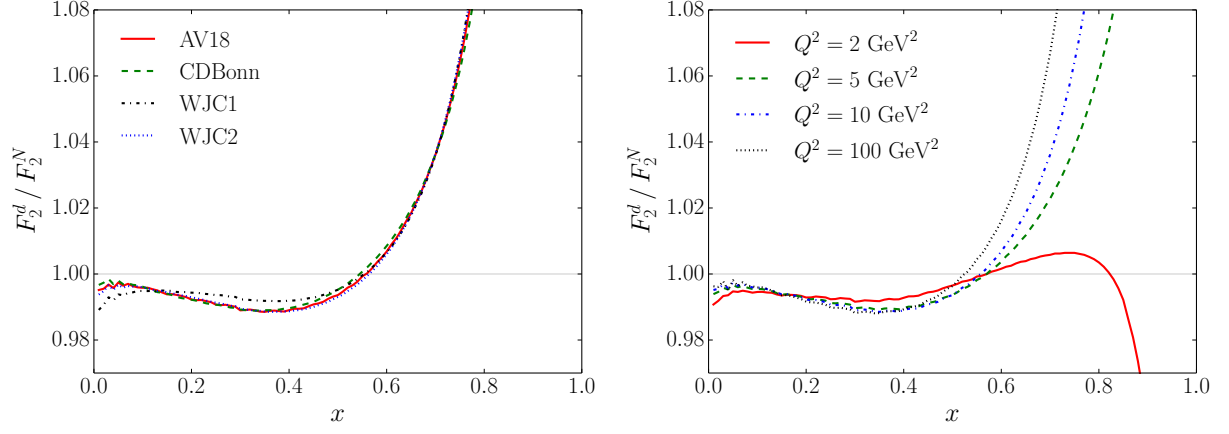


FIG. 5: Ratio of deuteron to isoscalar nucleon structure functions  $F_2^d / F_2^N$  for **(a)** different deuteron wave function models at  $Q^2 = 10 \text{ GeV}^2$ , and **(b)** different values of  $Q^2$  for the AV18 wave function.

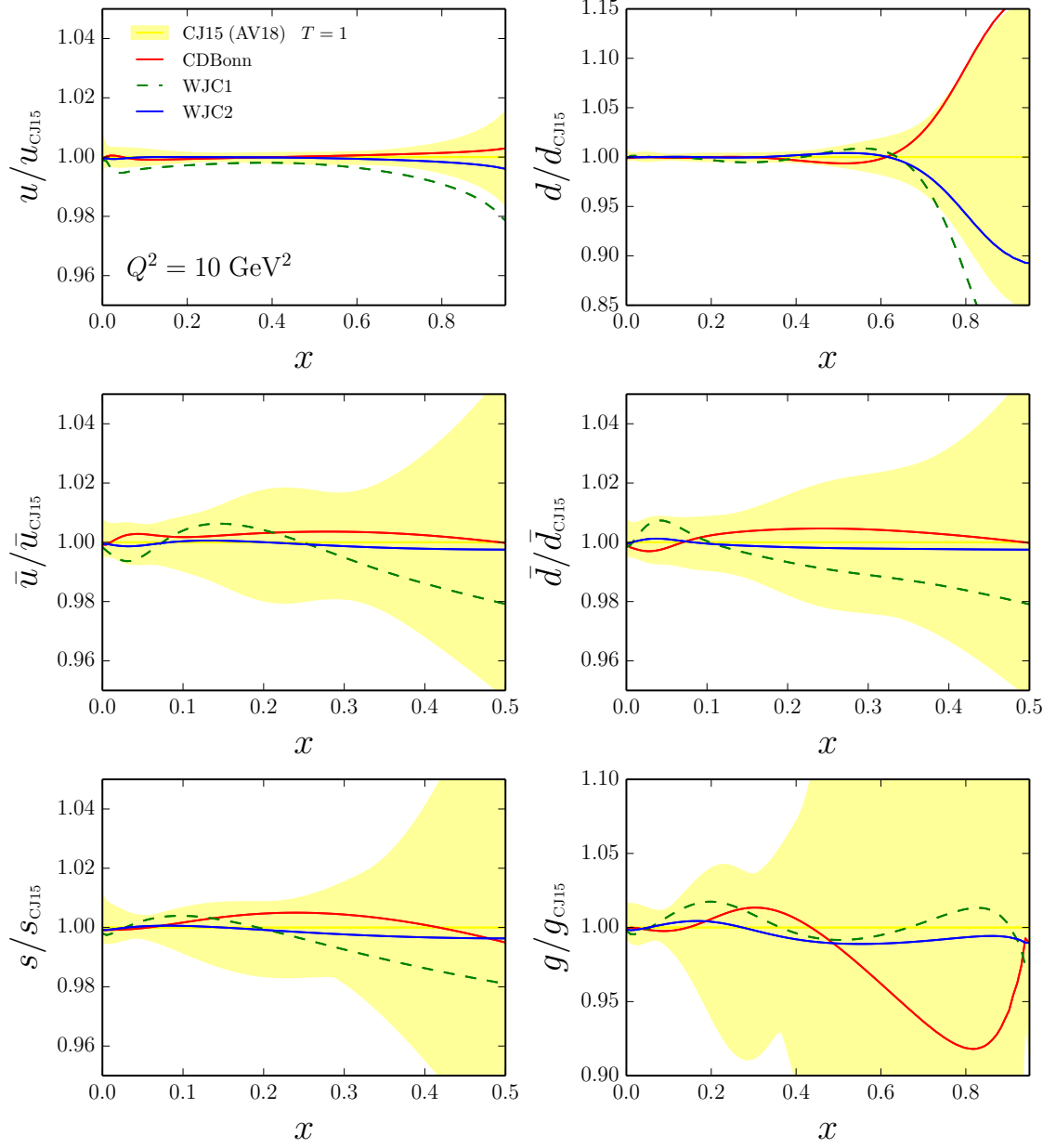


FIG. 6: Ratio of PDFs fitted using various deuteron wave function models to the CJ15 PDFs (which use the AV18 deuteron wave function): CD-Bonn (red solid lines), WJC-1 (green dashed lines), WJC-2 (blue solid lines). The CJ15 PDFs (yellow band) are shown for  $T = 1$ , and the off-shell parametrization (12) is used for all cases. Note the different scale on the vertical axes for the  $d$ -quark and gluon distributions.

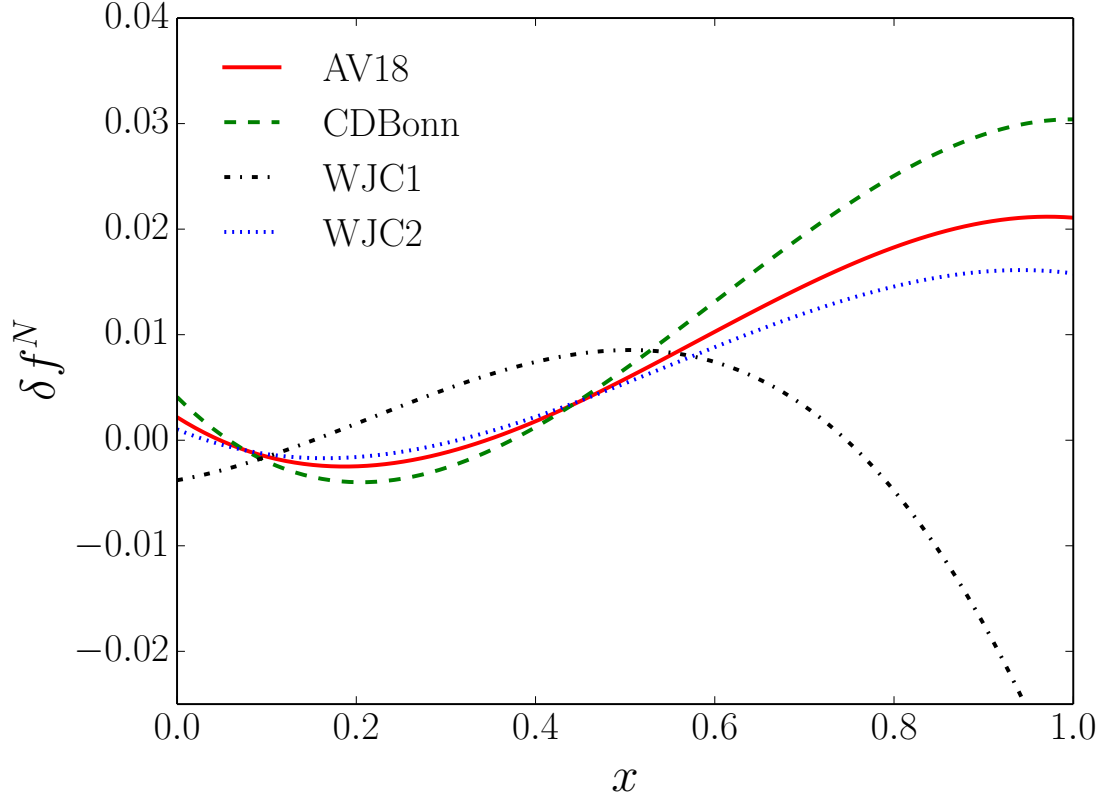


FIG. 7: Fitted nucleon off-shell correction  $\delta f^N$  for the parametrization in Eq. (12), using the AV18 (solid line), CD-Bonn (dashed line), WJC-1 (dot-dashed line) and WJC-2 (dotted line) wave functions.

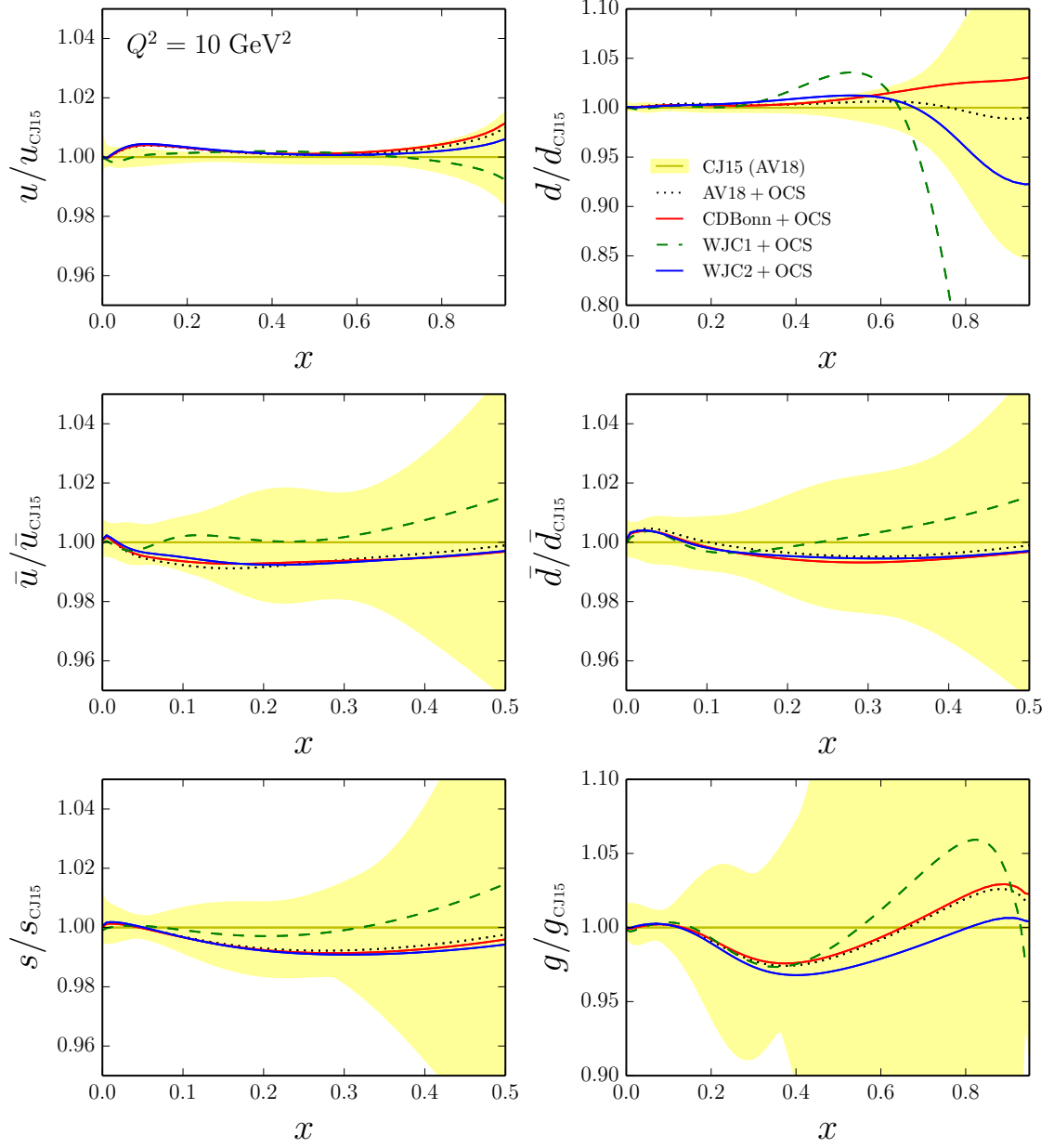


FIG. 8: Ratio of PDFs computed using the off-shell covariant spectator (OCS) model and different deuteron wave functions to the CJ15 PDFs (which use the off-shell parametrization (12) and the AV18 deuteron wave function): OCS model with the AV18 wave function (black dotted lines), CD-Bonn (red solid lines), WJC-1 (green dashed lines), and WJC-2 (blue solid lines). Note the different scale on the vertical axes for the  $d$ -quark and gluon distributions.



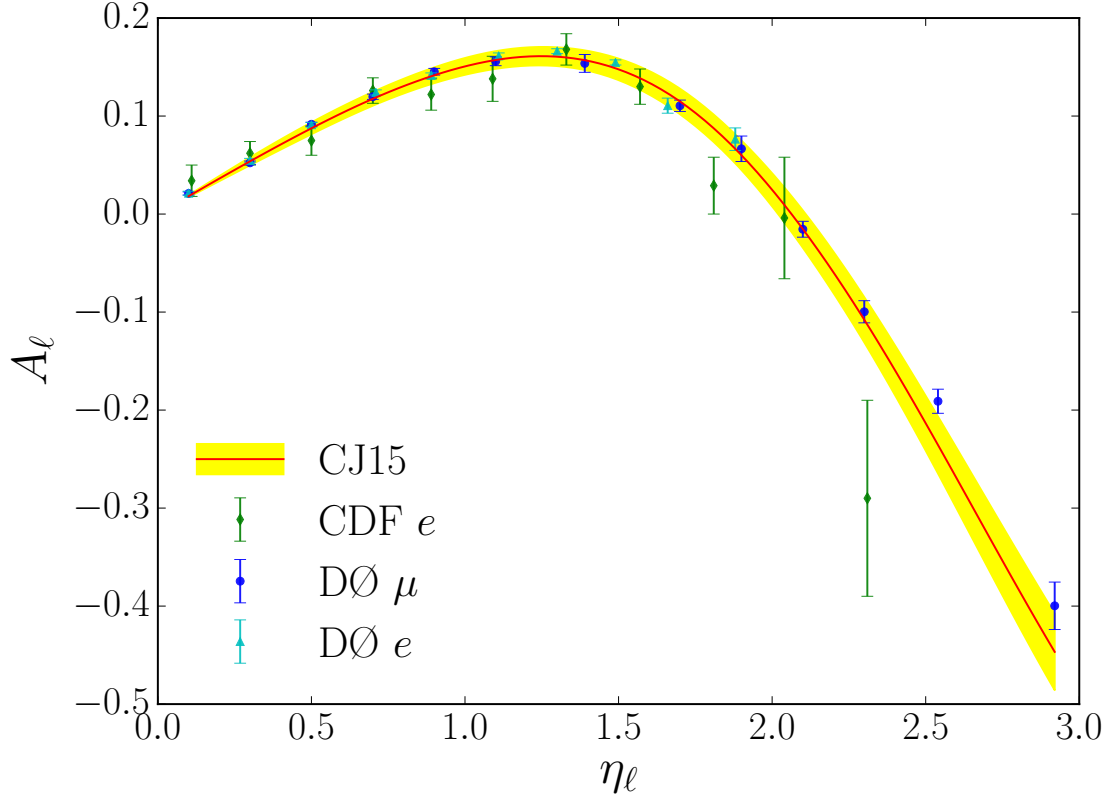


FIG. 9: Lepton charge asymmetry  $A_\ell$  from  $p\bar{p} \rightarrow WX \rightarrow \ell\nu X$  as a function of the lepton pseudo-rapidity  $\eta_\ell$  from CDF electron (green diamonds) [30], and DØ muon (blue circles) [31] and electron (cyan triangles) [32] data compared with the CJ15 fit.

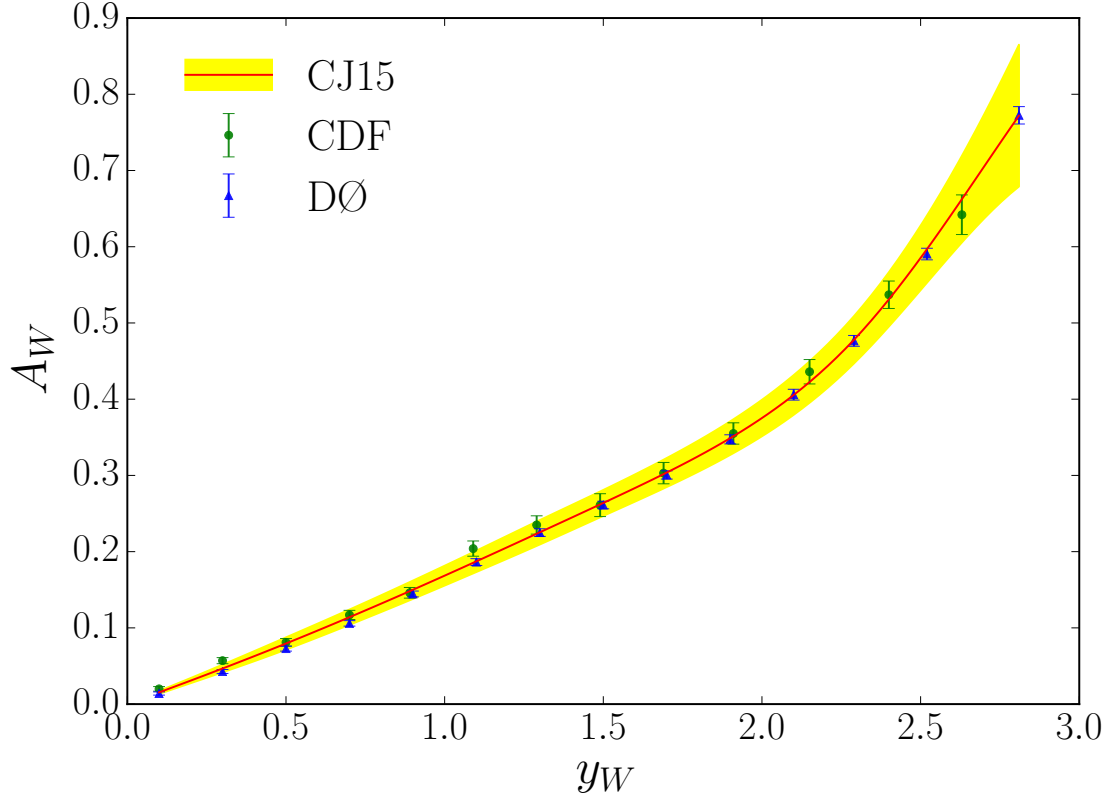


FIG. 10:  $W$  boson charge asymmetry  $A_W$  from  $p\bar{p} \rightarrow WX$  as a function of the  $W$  boson rapidity  $y_W$  for CDF (green circles) [33] and DØ (blue triangles) [34] data compared with the CJ15 fit.

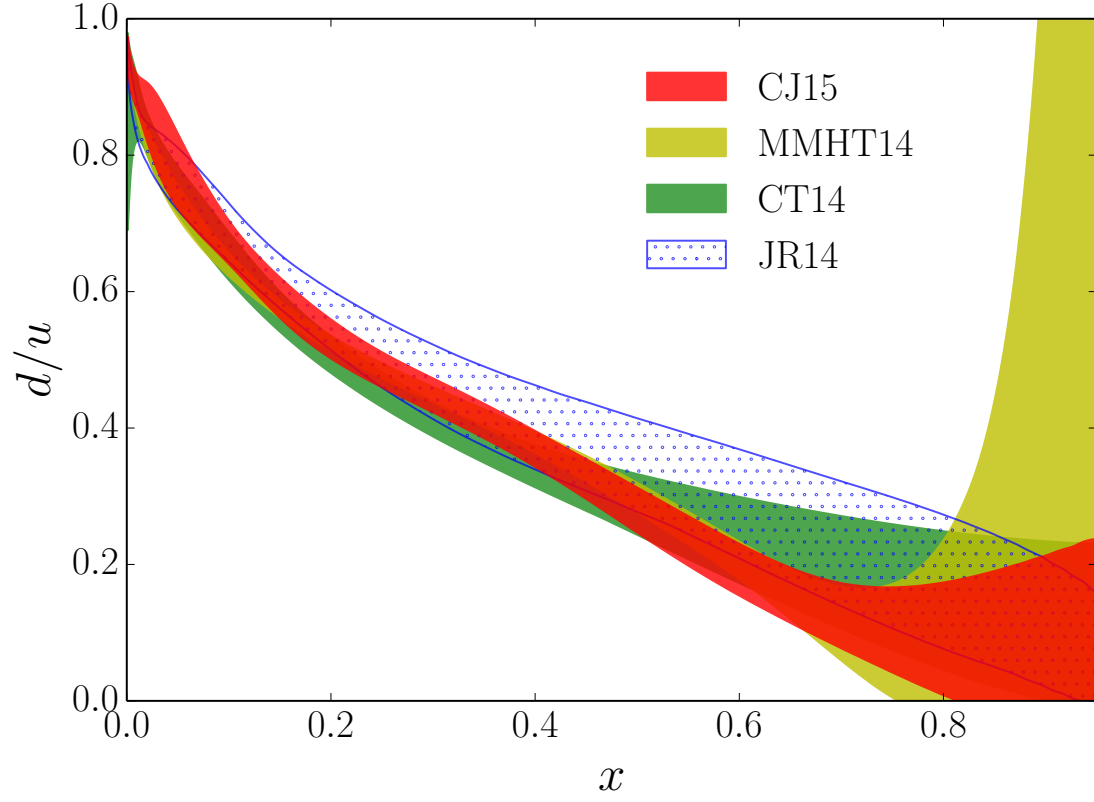


FIG. 11: Comparison of the  $d/u$  ratio at  $Q^2 = 10 \text{ GeV}^2$  for different PDF parametrizations: CJ15 (red band), MMHT14 [17] (yellow band), CT14 [18] (green band), and JR14 [47] (blue dotted band).

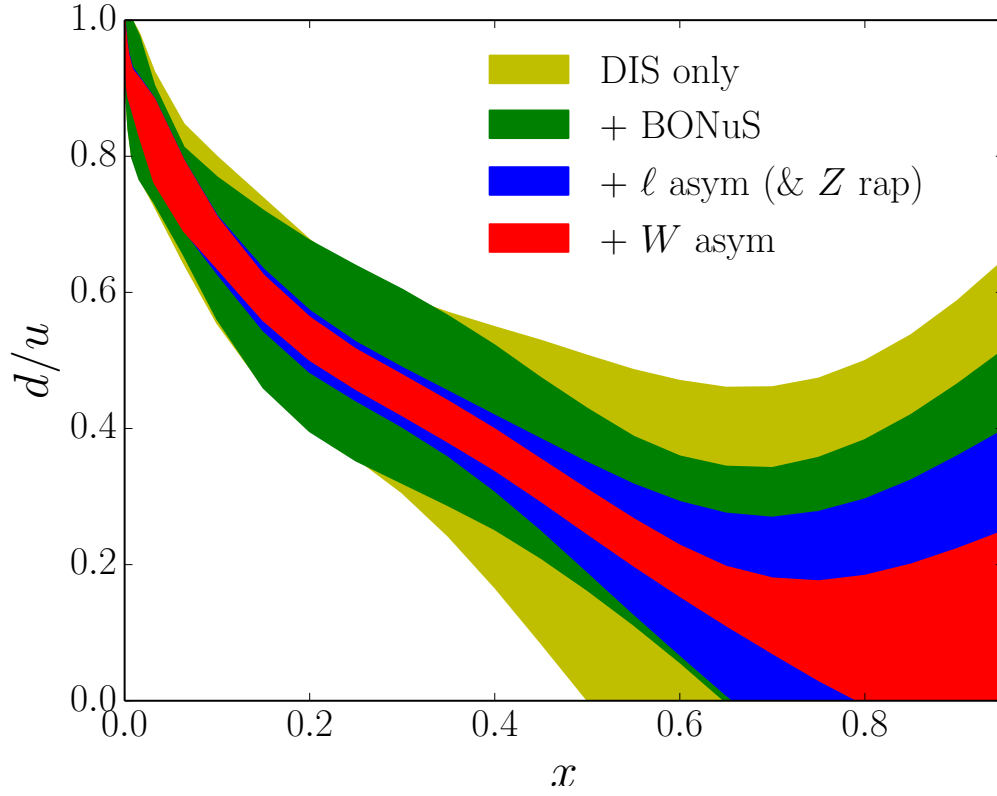


FIG. 12: Impact of various data sets on the  $d/u$  ratio at  $Q^2 = 10 \text{ GeV}^2$ . The uncertainty band is largest for the DIS only data (yellow band), and decreases with the successive addition of JLab  $F_2^n/F_2^d$  [83] data (green band), lepton asymmetry [30–32] (and  $Z$  rapidity [35, 36]) data (blue band), and  $W$  boson asymmetry data [33, 34] (red band). ...[FIGURE NEEDS SMOOTHING]...

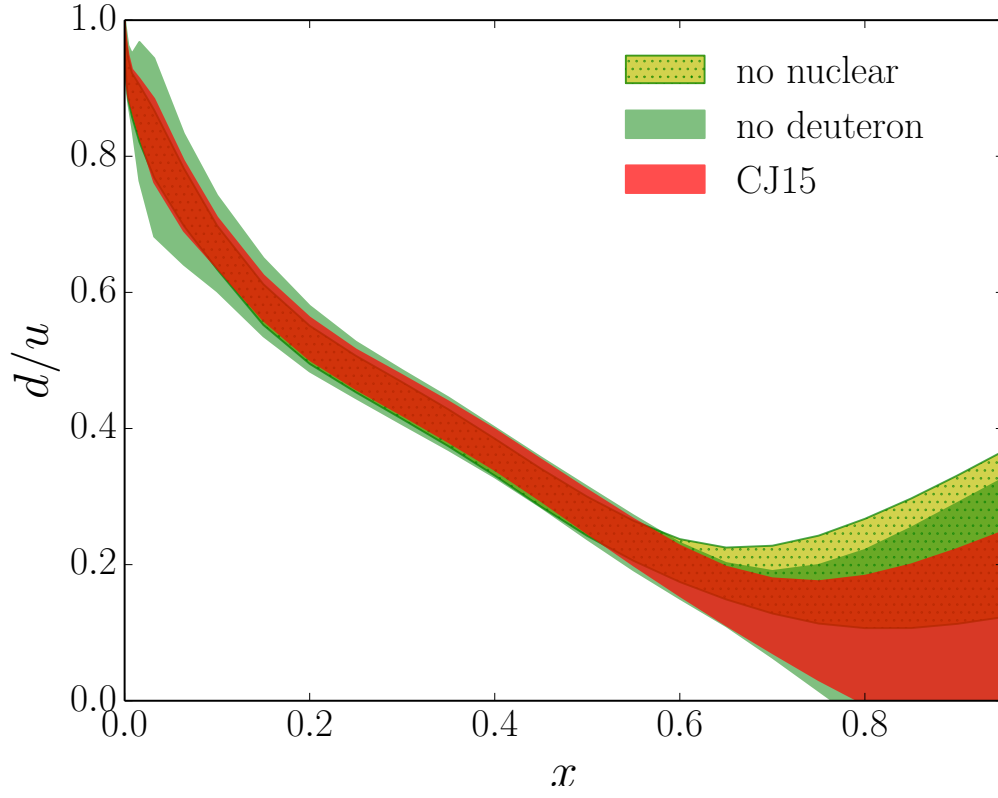


FIG. 13: Impact on the CJ15  $d/u$  ratio (red band) of removing the deuterium nuclear corrections (yellow shaded band), and omitting the deuterium data (green band). ...[FIGURE NEEDS SMOOTHING]...

TABLE I: Data sets used in the CJ15 global analysis, at NLO and LO, with the corresponding number of data points and the respective  $\chi^2$  values for each set.

	experiment	# points	$\chi^2$	
			NLO	LO
DIS $F_2$	BCDMS ( $p$ ) [22]	351	437	432
	BCDMS ( $d$ ) [22]	254	294	299
	NMC ( $p$ ) [23]	275	407	414
	NMC ( $d/p$ ) [24]	189	172	180
	SLAC ( $p$ ) [25]	564	435	496
	SLAC ( $d$ ) [25]	582	372	417
	JLab ( $p$ ) [26]	136	166	164
	JLab ( $d$ ) [26]	136	124	127
	JLab ( $n/d$ ) [83]	191	217	224
DIS $\sigma$	HERA (NC $e^-p$ ) [27]	145	112	161
	HERA (NC $e^+p$ ) [27]	408	541	872
	HERA (CC $e^-p$ ) [27]	34	19	19
	HERA (CC $e^+p$ ) [27]	34	31	33
Drell-Yan	E605 ( $p\text{Cu}$ ) [44]	119	93	104
	E866 ( $pp$ ) [28]	121	139	155
	E866 ( $pd$ ) [28]	129	144	191
	E866 ( $pd/pp$ ) [29]	12	9	9
$W$ /charge asymmetry	CDF ( $e$ ) [30]	11	12	11
	DØ ( $\mu$ ) [31]	10	20	21
	DØ ( $e$ ) [32]	13	27	56
	CDF ( $W$ ) [33]	13	15	12
	DØ ( $W$ ) [34]	14	16	47
$Z$ rapidity	CDF ( $Z$ ) [35]	28	27	79
	DØ ( $Z$ ) [36]	28	16	23
jet	CDF (run 2) [38]	72	15	22
	DØ (run 2) [40]	110	21	46
$\gamma$ +jet	DØ 1 [41]	16	6	20
	DØ 2 [41]	16	15	40
	DØ 3 [41]	12	25	35
	DØ 4 [41]	12	13	77
total		4035	3941	4786
total + norm			3950	4918
$\chi^2/\text{dof}$			0.979	1.219

TABLE II: Leading twist parameter values for the  $u_v$ ,  $d_v$ ,  $\bar{d} + \bar{u}$ ,  $\bar{d} - \bar{u}$  and  $g$  PDFs [Eq. (1)] from the CJ15 NLO analysis at the initial scale  $Q_0$  GeV. Parameters without errors have been fixed. For the strange to non-strange sea quark PDF ratio [Eq. (4)], we take  $\kappa = 0.4$ . (The parameter values are given to 5 significant figures to avoid rounding errors.)

parameter	$u_v$	$d_v$	$\bar{d} + \bar{u}$	$\bar{d} - \bar{u}$	$g$
$a_0$	2.3585	23.233	$0.14121 \pm 0.0050459$	35712	46.706
$a_1$	$0.60985 \pm 0.020299$	$1.1387 \pm 0.034586$	$-0.21785 \pm 0.0039454$	$3.9867 \pm 0.049301$	$0.61586 \pm 0.038277$
$a_2$	$3.5377 \pm 0.011405$	$6.6180 \pm 0.15977$	$8.4003 \pm 0.14833$	$20.289 \pm 0.66322$	$6.2335 \pm 1.1222$
$a_3$	0	$-3.5743 \pm 0.090782$	0	17	$-3.2703 \pm 0.16746$
$a_4$	$3.5169 \pm 0.42791$	$4.9133 \pm 0.14586$	$16.055 \pm 1.1403$	$49.881 \pm 7.1398$	$3.0338 \pm 0.31300$
$b$	—	$-0.0042424 \pm 0.00070691$	—	—	—
$c$	—	2	—	—	—

TABLE III: Higher twist parameters [Eq. (6)] and nucleon off-shell parameters [Eq. (12)] from the CJ15 NLO analysis at the input scale  $Q_0$ . Parameters without errors have been fixed. (The parameter values are given to 5 significant figures to avoid rounding errors.)

parameter	value
$h_0$	$-3.0094 \pm 0.24080$
$h_1$	$1.7526 \pm 0.10135$
$h_2$	$-2.0895 \pm 0.026853$
$C_0$	$0.098222 \pm 0.028518$
$x_0$	$0.34487 \pm 0.91982$
$x_1$	0.048